Scientific African 22 (2023) e01943

Contents lists available at ScienceDirect

Scientific African

journal homepage: www.elsevier.com/locate/sciaf

Antiproliferative activity of ethyl acetate fraction of *Euphorbia ingens* against prostate cancer cell line: An *in silico* and *in vitro* analysis

Innocent Oluwaseun Okpako [a,*], Florence Atieno Ng'ong'a [b], Cleophas Mutinda Kyama [c], Sospeter Ngoci Njeru [d]

[a] *Department of Molecular Biology and Biotechnology, Pan African University Institute for Basic Sciences, Technology and Innovation, Nairobi, Kenya*
[b] *Department of Biochemistry, School of Biomedical Sciences, College of Health Sciences, Jomo Kenyatta University of Agriculture and Technology, Nairobi, Kenya*
[c] *Department of Medical Laboratory Sciences, School of Biomedical Sciences, College of Health Sciences, Nairobi, Kenya*
[d] *Centre for Traditional Medicine and Drug Research, Kenya Medical Research Institute, Nairobi, Kenya*

ARTICLE INFO

Editor: DR B Gyampoh

Keywords:
Phytochemicals
Cytotoxicity
Anticancer
Treatment
Network pharmacology
Molecular targets

ABSTRACT

Current prostate cancer (PCa) treatments often lead to severe side effects, prompting the exploration of safer alternatives. *Euphorbia ingens* is a medicinal plant used for cancer treatment in African communities; however, there is no scientific validation of its anticancer activity. This study therefore evaluated the antiproliferative activity of *E. ingens* on the DU-145 human PCa cell line. The 3-[4,5-dimethylthiazol-2-yl]-2,5-diphenyltetrazolium bromide (MTT) bio-assay was used to determine the antiproliferative activity of *E. ingens* ethyl acetate-, and water-fractions. Only the ethyl acetate fraction was considered to be active. It inhibited DU-145 cell growth selectively without toxicity to non-cancerous Vero E6 cells. The IC_{50} was 9.71 ± 0.4 µg/ml and had a selectivity index of 8.26, indicating promising efficacy and cellular safety. Qualitative phytochemical screening identified the presence of phenols, terpenoids, flavonoids, tannins, sterols, and saponins in the ethyl acetate fraction. An additional 18 chemical compounds with potential synergistic roles were identified through gas chromatography-mass spectrometry analysis. Network pharmacology was then employed to predict molecular targets and mechanisms of action for drug-like chemical compounds, implicating key targets such as ESR1, IL6, MMP9, CDK2, MAP2K1, AR, PRKCD, CDK1, CDC25B, and JAK2 with regulation of PI3K/Akt, MAPK, and p53 signaling pathways suggested to be the potential mechanism of action. Further, gene expression analysis of selected targets through reverse transcription-quantitative polymerase chain reaction revealed downregulation of AR and BCL2 levels, along with upregulation of p53 and caspase-3 in fraction-treated DU-145 cells compared to the 0.2 % DMSO-negative control. In conclusion, the findings of this study validate the traditional use of *E. ingens* in cancer management. The identified drug-like compounds, their targets, and associated signaling pathways could serve as a foundation for developing novel strategies for prostate cancer management. However, we recommend additional *in vitro* and *in vivo* studies to further substantiate these findings.

* Corresponding author.
E-mail addresses: innocentokpako9@gmail.com (I.O. Okpako), snjeru@kemri.go.ke (S.N. Njeru).

https://doi.org/10.1016/j.sciaf.2023.e01943
Received 13 July 2023; Received in revised form 11 October 2023; Accepted 13 October 2023
Available online 14 October 2023

Introduction

Cancer is one of the major causes of death globally and a significant contributor to decreased life expectancy. Cancer of the prostate is an adenocarcinoma that often forms in the glandular prostate, it can remain contained in the prostate for a long time or advance by metastasizing outside the prostate. According to the World Health Organization (WHO), in 2020, there were 1414,259 new cases of prostate cancer (PCa); it is the second most common cancer in men and the fifth most significant cause of cancer-related mortality globally [1]. Due to a lack of effective preventive and treatment strategies, data in 2020 show that 77,300 new cases were estimated to have occurred in sub-Saharan Africa [2].

Prostatectomy and local radiation are used to treat localized PCa, which accounts for 90% of PCa cases. However, PCa is diagnosed at an advanced stage in around 90% of men with the disease. The common treatment options for advanced PCa are androgen deprivation therapy (ADT) and chemotherapy. ADT treatment leads to recurrent androgen-independent prostate cancer within 2–3 years, with frequent metastases to regional lymph nodes or the pelvis. Although there are several prostate cancer chemotherapy treatments, there is still a knowledge gap on the evolution of treatment interventions resistance coupled with limited evidence of the therapeutic options for advanced prostate cancer. Drugs that target rapidly proliferating cancer cells, such as docetaxel and paclitaxel, can also damage healthy cells, causing fatigue, hypertension, hot flushes, arthralgia, fractures, peripheral edema, and rash. Therefore, there is an urgent need for better therapeutic interventions against PCa, and herbal plant sources provide the greatest promise and the "lowest hanging fruits".

The use of herbal plants in cancer has gained substantial attention, and recently, ongoing research with the US National Cancer Institute (NCI) have played a pivotal role in promoting the use of traditional medicine to treat cancer [3]. Herbal plants have various advantages over chemical products due to their lower chances of inducing adverse effects, cost-effectiveness, tolerability, and reduced chances of developing resistance. Plants exercise their anticancer properties owing to the existence of phytochemicals that act by combating lipid peroxidation through their anti-oxidative properties, repairing damaged DNA, boosting the immune system, inducing apoptosis, and suppressing the cell cycle [4].

Euphorbia ingens E. mey. ex Boiss belongs to the plant family *Euphorbiaceae*. It is known to contain latex; the leaves, stem, root, and whole plant are applied in traditional medicine for the treatment of cancer and other pathologies, including swellings, fistula, lesions, wounds, abscesses, burns and mental disorders [5,6]. In East Africa, *E. ingens* is also used for the treatment of snakebites, suggesting that the plant may possess an anti-venom property. Additionally, there are scientific data demonstrating the ichthyoidal, antitubercular, antimicrobial, and antifungal activities of *E. ingens* [7–9]. However, despite the aforementioned roles of *E. ingens* as a viable therapeutic option for the management and treatment of diseases in ethnomedicine, there is no scientific validation of its ethnobotanical use in cancer management, and treatment. In this context, we hypothesized that *E. ingens* could selectively abrogate the proliferation of prostate cancer cells.

Various plant parts, including stems, leaves, bark, fruits, and seeds, are employed in the formulation of cancer treatments; the roots, as highlighted by Koduru et al. [6], are mostly used. Also, previous studies have reported *E. ingens*' stems and leaves to be inactive against human hepatoma, human breast adenocarcinoma, and human colon adenocarcinoma cell lines [10]. To test our hypothesis, we prepared crude (dichloromethane-methanol (1:1, v/v)) extract, hexane-, ethyl acetate-, and water-fractions from the roots of *E. ingens*, assessing their inhibitory effects on DU-145 prostate cancer cells. Subsequently, we evaluated the cellular safety of the ethyl acetate fraction—identified for its robust antiproliferative activity—in non-cancerous Vero E6 cells. Employing network pharmacology, we probed the likely molecular targets and anticancer mechanisms of action associated with the chemical compounds identified within the efficacious ethyl acetate fraction. Using reverse transcription-quantitative polymerase chain reaction (RT-qPCR), we determined the gene expression levels of selected molecular targets and genes known to play pivotal roles in prostate cancer initiation and progression. Collectively, our study scientifically validates the traditional use of *E. ingens* in treating and managing cancer, positioning the plant as a promising source for discovering bioactive compounds tailored for the treatment and/or management of prostate cancer. This is in line with Sustainable Development Goal 3, Target 3.4, which aims to reduce the mortality rate attributed to cancer by one-third by 2030. It is worthy of note that the goal coincides with goal 3 of Africa Agenda 2063, an aspiration to achieve a population that is healthy and well-nourished across the African continent.

Materials and methods

Plant collection and processing

Fresh root samples of *E. ingens* were obtained on March 26, 2022, from Embu County, Kenya (0° 46′ 27.0″ South, 37° 40′ 54.9″ East), where it grows naturally. Plant identification and authentication were carried out at Egerton University, Kenya by a plant taxonomist, and a voucher specimen number NSN9 was subsequently deposited in the same place. Approximately 2 kg of plant roots were carefully taken, washed thoroughly with water to remove sand and any other contaminants. They were cut into little pieces and shade dried at room temperature for 21 days, with the samples regularly turned upside down to avoid fungal growth. The dried samples were then milled into fine powder using an electric grinder (Christy 8 MILL, serial number 51,474). The powder of *E. ingens* (411 g) was soaked in a volume of 1 L of dichloromethane-methanol (1:1, v/v) solvent. Following percolation and intermittent agitation, the resulting liquid was filtered with Whatman No. 1 filter paper. This was done repeatedly until the initial deep color of the filtrate faded to indicate an exhaustive solvent extraction. The filtrate was successively evaporated to dryness at 57 °C using a 5-liter rotary vacuum evaporator (Rotavapor R-300; Buchi, Switzerland). The obtained extract was 149 g and the yield percentage were calculated using the following

equation:

Percentage yield of extracts = [(Weight of the obtained extract material/Weight of original fine plant powder used)* 100]

The crude extract was further partitioned into hexane, ethyl acetate, and water fractions as previously described by Beesoo et al. [11] with slight modification. The dichloromethane and methanol mixture was used to establish an intermediate polarity between the non-polar and polar solvents, which allowed for the extraction of a significant quantity of chemical compounds [12]. Hexane, ethyl acetate, and water were used to purify and concentrate non-polar compounds in hexane and polar ones in ethyl acetate and water. Also, *Euphorbia* species are known to be rich in essential oils and fats, and hexane, ethyl acetate, and water are defatting solvents [13].

20 g of dried crude extract were weighed and dissolved in 50 ml of a 1:1 solution of dichloromethane and methanol. In a separating funnel, 300 ml of hexane was vigorously mixed through shaking with the solution that was made. The mixture was then left undisturbed for 30 min to ensure proper separation. The upper hexane part was then decanted in a beaker. This was done two more times to ensure complete partitioning of the hexane fraction. The process continued by introducing 300 ml of ethyl acetate and distilled water (1:1) into the remaining lower part, from which the hexane fraction was washed off. The ethyl acetate fraction settled atop the distilled water part, and the two layers were collected separately in beakers. The collected hexane and ethyl acetate fractions were concentrated by the rotary vacuum evaporator, while the water part was taken for freeze drying. Following partitioning, the crude and obtained hexane, ethyl acetate, and water fractions were stored at −20 °C until further analysis.

Cell culture

A human prostate carcinoma cell line (DU-145) and a kidney epithelial cell line derived from African green monkeys (Vero E6) were purchased from the American Type Culture Collection (ATCC) and cultured at the Kenya Medical Research Institute's center for Traditional Medicine and Drug Research. The cells were grown in Modified Eagle's Medium (MEM, Sigma-Aldrich, USA) supplemented with 1 % L-glutamine (200 mM) (Sigma-Aldrich, USA), 10 % fetal bovine serum (FBS, Gibco, USA), 1.5 % sodium bicarbonate (Loba chemie, India), 1 % HEPES (1 M) (GoldBio, USA), and 1 % penicillin-streptomycin (Sigma-Aldrich, USA), at 37 °C and 5 % CO_2. The DU-145 cell line was selected as it has moderate metastatic potential, while Vero E6 is the non-cancerous cell (employed to assess the cellular toxicity of the plant's fraction) [14,15]. The passage numbers of the DU-145 and Vero E6 cell lines used in this study were 30 (DU145HTB-81/P-30/06/22) and 14 (VeroE6/P-14/08/22), respectively; and were sub-cultured twice a week. The logarithmic growth phase of the cells was used in all studies.

Cellular proliferation assay

The 3-[4,5-dimethylthiazol-2-yl]−2,5-diphenyltetrazolium bromide (MTT) assay was used to test how well the plant fractions stopped cell growth. The DU-145 cells at 80 % confluence were washed with phosphate buffered saline (PBS, Sigma-Aldrich, USA) and detached by a 0.25 % trypsin-ethylenediaminetetraacetic acid (trypsin-EDTA) solution (Solarbio, China). 100 µl of cell suspensions was taken into a sterile Eppendorf tube, and 50 µl of trypan blue (Loba chemie, India) was added and mixed. The hemocytometer was then used to count the number of viable cells. Cell suspensions with a cell density of 1×10^4 cells/well were seeded onto flat-bottomed 96-well plates and grown for 24 hours. A stock solution of 100,000 µg/ml was prepared by dissolving 30 µg of plant fractions in 300 µl of 100 % dimethyl sulfoxide (DMSO, Finar Chemicals, India) and diluted appropriately with growth medium so that the final concentration of DMSO in the test sample is 0.2 %. The seeding medium was aspirated from the plates, and 100 µl of a 200 µg/ml (in culture medium) working concentration of plant fractions were added for 48 h as screening treatments. The same concentration of doxorubicin (Solarbio, China) was used as a positive control, while 0.2 % DMSO was used as a negative control. After 48 h of exposing the cells to the treatments, 10 µl of freshly prepared MTT (5 mg/ml) was added to each well and incubated for 4 hours. Following that, MTT was aspirated out, and 100 µl of 100 % DMSO was added to solubilize the formazan crystals. Then, using the absorbance at 570 nm, a plate reader (an Infinite M1000 by Tecan) read the 96-well plates. Experiments were carried out in triplicate, and the percentage cell survival was calculated using the formula [14]:

Percentage cell viability = [(Absorbance of treated cells –Absorbance of culture medium/Absorbance of untreated cells –Absorbance of culture medium) * 100]

After the initial screening at a single concentration (200 µg/ml), the fractions with equal or less than 50 % cell viability after 48 h of treatment were considered active and selected for further antiproliferative studies using a range of concentrations (6.25–200 µg/ml) [16]. The 50 % inhibition concentration (IC_{50}) was then determined. The cytotoxicity of the E. ingens fraction was further assessed on Vero E6 cells using the MTT cell proliferation assay previously described, and the 50 % cytotoxicity concentration (CC_{50}) was calculated.

Selectivity index

The selectivity index (SI) for the tested plant fraction and doxorubicin was determined by dividing the IC_{50} by the corresponding CC_{50}.

Identification of plant compounds

The plant fraction that showed antiproliferative activity was subjected to qualitative phytochemical screening and gas chromatography-mass spectrometry (GC–MS) analysis. This was to identify the class of compounds as well as the specific compounds that may be responsible for the observed bioactivity.

Qualitative phytochemical screening

Qualitative phytochemical screening was done for the presence of alkaloids, terpenoids, flavonoids, sterols, tannins, saponins, quinones and phenols as highlighted by Shaikh & Patil [17].

Tests for alkaloids (Dragendorff's test): 1 ml of Dragendorff's reagent was added to 2 ml of plant fraction. The formation of a brownish-red color indicates the presence of alkaloid.

Test for terpenoids (Salkowki's test): 1 ml of chloroform (Scharlau, Spain) was added to 2 ml of fraction, then a few drops of concentrated sulfuric acid (H_2SO_4, HPLC, India). An immediate production of a gray color signifies the presence of terpenoid.

Test for flavonoids (alkaline reagent test): 2–3 drops of sodium hydroxide (NaOH, BDH chemicals Ltd Poole, England) were added to 2 ml of fraction. The presence of flavonoid is indicated by a deep yellow color appearance that would gradually become colorless by introducing a few drops of dilute (5 %) hydrochloric acid (HCl).

Test for sterols (Liebermann-Burchard test): 2 ml of fraction was treated with 2 ml of chloroform, 10 drops of acetic anhydride, and 2 drops of concentrated H_2SO_4. The formation of a dark pink or red color confirms the presence of sterols.

Test for tannins (Braymer's test): A volume of 2 ml of fraction was treated with a methanolic solution of ferric chloride (10 %) (GriffChem, India). Tannins are present when there is the formation of a blue- or greenish-colored solution.

Test for saponins (foam test): 2 ml of fraction was added to 6 ml of water in a test tube and shaken vigorously. An appearance of persistent foam indicates the presence of saponins.

Test for quinones (concentrated HCl test): A volume of 2 ml of fraction was treated with concentrated (98 %) HCl. The formation of a green color is an indication of the presence of quinones.

Test for phenols (ferric chloride test): A volume of 2 ml of the fraction was treated with aqueous 5 % ferric chloride. Phenols are confirmed when there is production of a deep blue or black color.

Gas chromatography-mass spectrometry analysis

Further identification of specific chemical compounds was carried out using a gas chromatography mass spectrometer system (Model; Shimadzu, GC–MS QP-2010SE) and a low polarity BPX5 capillary column (30 $m \times 0.25$ mm $\times$ 0.25 μm film thickness). The oven temperature was programmed to commence at 55 °C and remain constant for 1 min before increasing by 10 °C per minute until it reached its isothermal temperature of 280 °C with a final hold time of 15 min and 30 s. The injector was maintained at 200 °C; at a constant rate of 1.08 ml/min, helium was utilized as a carrier gas. The solvent delay was 4 min, and 1 μl diluted sample was automatically injected using an AS3000 autosampler coupled with GC in split mode, split ratio (10:1). The temperature of the ion source and interface was set to 200 °C and 250 °C, respectively. Over the range of m/z 35–550, EI mass spectra were collected at 70 eV in full scan mode. For the qualitative identification of compounds found in the extract, the NIST mass spectral database was utilized.

In silico work

Drug candidate screening test

The Canonical SMILES (Simplified Molecular Input Line Entry System) of the GC–MS identified compounds in the active fraction were retrieved from PubChem (https://pubchem.ncbi.nlm.nih.gov/). The SMILES were then submitted to the Swiss ADME (absorption, distribution, metabolism, and excretion) tool (http://www.swissadme.ch/index.php) to predict the drug-likeness and physicochemical properties of the compounds. The prediction was based on the parameters of the blood-brain barrier, total polar surface area, cytochrome P450s (CYP2D6 and CYP3A4), and Lipinski's rule of five (RO5) (a drug candidate should have a molecular weight of fewer than 500 g/mol, a number of rotatable bonds of less than 10, a number of hydrogen bond donors of less than 5, a number of hydrogen bond acceptors of less than 10, and a lipophilicity (log P) value of less than 5). It was predicted that a molecule would be a non-orally accessible medicine if two or more of the RO5 were not met [18].

The polar atoms of a molecule add up to the topological polar surface area (TPSA), which can be used to predict how the drug will be transported. In most cases, the amount of TPSA in an approved medicine was below 140 $Å^2$ [19]. Substances that are able to breach the blood-brain barrier can be hazardous to the nervous system because they can pass from the more hydrophilic blood to the more lipophilic brain. A drug candidate should not block cytochrome P450 enzymes (such as CYP2D6 and CYP3A4) because they are essential for drug metabolism [19].

Identification of candidate targets in E. ingens against PCa

Compound targets were predicted using BindinDB (https://bindingdb.org/rwd/bind/chemsearch/marvin/FMCT.jsp) correspondence to known ligand molecules having a minimum similarity of > 0.7, and their Gene IDs were retrieved from the UniProtKB (https://www.uniprot.org) database. Similarly, the SMILES of the compounds were uploaded to the Swiss TargetPrediction (http://www.swisstargetprediction.ch/)database, with "humans" (Homo sapiens) as the study species, and the probability of each potential target was determined to be >0. The retrieved targets were converted into standardized abbreviations by UniProt. The resulting predicted compound targets from the two databases were pooled together, and duplicates were removed. Disease targets for PCa were

collected from the GeneCards (https://www.genecards.org/) and DisGeNET (https://www.disgenet.org/) databases. The targets from the databases were searched using the keyword "prostate cancer." The retrieved results were merged to ensure there were no repeats. Finally, the targets of active compounds of *E. ingens* and disease targets of PCa were intersected using the bioinformatics and evolutionary genomics platform (https://bioinformatics.psb.ugent.be/webtools/Venn/).

Construction of the protein-protein interaction (PPI) network

Protein-protein interaction (PPI) networks are the physical connections established between proteins within a cell, either through biochemical reactions or biological processes. The intersections obtained, which are considered the common potential targets, were uploaded to the STRING 11.5 database (https://string-db.org/) to establish a PPI network so as to explore the interaction between the targets. The species was set as "*Homo sapiens*", and the minimum interaction threshold was set to 0.4. The Cytohubba plug-in Cytoscape software (version 3.9.1) was used to analyze the topology of the network, and the Maximal Clique Centrality (MCC) algorithm was used to filter out the top 10 key targets. Proteins that stick closely together in a protein network are considered the important ones. The MCC demonstrates a higher capacity for capturing crucial proteins in the top-ranked list, regardless of whether they are high-degree or low-degree proteins [20].

Gene ontology (GO) & kyoto encyclopedia of genes and genomes (KEGG) enrichment analysis

The GO provides information on the functions of genes; these include the biological process (BP), the cellular component (CC), and the molecular function (MF). Analysis of KEGG, on the other hand, is used to identify important pathways for gene enrichment. The GO and KEGG enrichment analyses for the targets of *E. ingens* for PCa treatment were conducted by submitting the gene IDs of the intersected common targets in the enrichment tool ShinyGO version 0.76 (http://ge-lab.org/go/). The following parameters were considered for the analyses: species = Human, false discovery rate (FDR) cut-off = 0.05, and number of pathways to show = 20.

Gene expression: reverse transcription-quantitative polymerase chain reaction (RT-qPCR)

Eighty percent (80 %) of the confluent DU-145 in a T-25 flask was treated with *E. ingen* fraction at a concentration equivalent to the calculated IC_{50}. Negative control cells were exposed to fresh growth media with 0.2 % DMSO. The cells were incubated for 48 h. Cells were collected for the extraction of total RNA, and reverse transcription was conducted using FIRE Script RT cDNA synthesis kit (Solis BioDyne, Estonia). Luna Universal qPCR Master Mix (New England Biolabs) was used for RT-qPCR detection. Table 1 shows the primers sequences that were used which were designed utilizing the National center for Biotechnology Information (NCBI) Primer Blast tool (https://www.ncbi.nlm.nih.gov/tools/primer-blast). β-actin served as the housekeeping gene. The fragment sizes ranged from 70 to 250 bps and had a 40–60% GC content and self-complementarity ≤ 2. The primer sequences (Macrogen Europe BV, Netherlands) are listed as follows:

Statistical analysis

GraphPad Prism version 8.4.0 software (San Diego, CA, USA) was used for statistical analysis. The data was presented as the mean ± standard error of the mean (SEM). An independent-sample T test was used for the comparison between two groups, and a one-way ANOVA was used for the comparison between multiple groups, and $p < 0.05$ was considered statistically significant.

Results

Plant extract preparation

The percentage yield of the dichloromethane-methanol root extract of *E. ingens* was 36.25 %. Of the four (crude dichloromethane-methanol, hexane, ethyl acetate, and water) fractions of *E. ingens* that were obtained after solvent partitioning, the crude and hexane

Table 1
Primers sequences.

Genes	Primers	Fragment Size (bp)
AR	Forward- GCTTTATCAGGGAGAACAGCCT	
	Reverse- TGCAGCTCTCTCGCAATCTG	198
BCL2	Forward- GGCCTCAGGGAACAGAATGAT	
	Reverse- TCCTGTTGCTTTCGTTTCTTTC	201
CDK1	Forward- GAACACCACTTGTCCCTCTAAGAT	
	Reverse- CTGCTTAGTTCAGAGAAAAGTGC	170
Caspase-3	Forward- CAAAGAGGAAGCACCAGAACCC	
	Reverse- GGACTTGGGAAGCATAAGCGA	89
P53	Forward- CTTCGAGATGTTCCGAGAGC	
	Reverse- GACCATGAAGGCAGGATGAG	181
β –Actin	Forward- GCCAACTTGTCCTTACCCAGA	
	Reverse- AGGAACAGAGACCTGACCCC	106

fractions dissolved sparingly in dimethyl sulfoxide (DMSO), and so they were not considered for further bioassays since accounting for their concentrations would not be possible.

Antiproliferative and cytotoxic activity

The ethyl acetate and water fractions were evaluated in a blind screening for their potential antiproliferative activity against DU-145 at a fixed concentration of 200 μg/ml (Fig. 1A). Only the ethyl acetate fraction displayed antiproliferative activity of >50 % at 200 μg/ml, and therefore, it was prioritized for concentration-dependent testing through 2-fold serial dilution. The inhibition of cell proliferation by the ethyl acetate fraction in a concentration-response-dependent manner against DU-145 is shown in Fig. 1B, whereby the IC_{50} of the fraction was calculated at 9.71 ± 0.4 μg/ml while the standard reference drug, doxorubicin, had an IC_{50} of 5.30 ± 0.11 μg/ml (supplementary figure 1). There was a significant ($p = 0.0115$) difference when the two treatments were compared (supplementary table 1). Images of the cells following treatment with the plant's fraction and doxorubicin are shown in supplementary figure 2. Subsequently, the fraction's *in vitro* safety was determined using non-cancerous Vero E6 cells (Fig. 1C). The cytotoxic concentration killing 50 % of treated cells (CC_{50}) of the *E. ingens* ethyl acetate was 80.19 ± 6.12, which is significantly ($p < 0.05$) different (supplementary table 1) from the doxorubicin drug (176.10 ± 8.09) (supplementary figure 3).

Selectivity index (SI)

The IC_{50} and CC_{50} values for the tested ethyl acetate fraction were determined from the data extracted in Figs. 2 and 3, respectively and for doxorubicin from supplementary figures 1 and 2, respectively, and the SI was calculated. Table 1 shows the summary of all the values, whereby the IC_{50} of 9.71 μg/ml and CC_{50} of 80.19 μg/ml of the ethyl acetate fraction of *E. ingens* gave an SI of 8.26; the SI calculated for doxorubicin for an IC_{50} of 5.30 μg/ml and CC_{50} μg/ml of 176.10 is 33.23.

Identification and analysis of E. ingens ethyl acetate bioactive compounds

Qualitative phytochemical screening

The results of the qualitative phytochemical screening to identify the class of compounds that, to some extent, could be responsible for the observed antiproliferative activity of the ethyl acetate fraction are shown in supplementary table 2. Tannins, terpenoids, flavonoids, saponins and sterols were found to be abundant, with phenol moderately present. Alkaloids and quinones were absent.

In-depth compounds characterization by gas chromatography–mass spectrometry (GC–MS)

To further identify the specific compounds that were present in the ethyl acetate fraction, GC–MS was used. The chromatogram of GC–MS spectra of compounds is shown in supplementary figure 4. The individual compound's identification was established on the basis of the peak area and retention time, and the details are presented in Table 2. Twenty-two peaks were observed in the

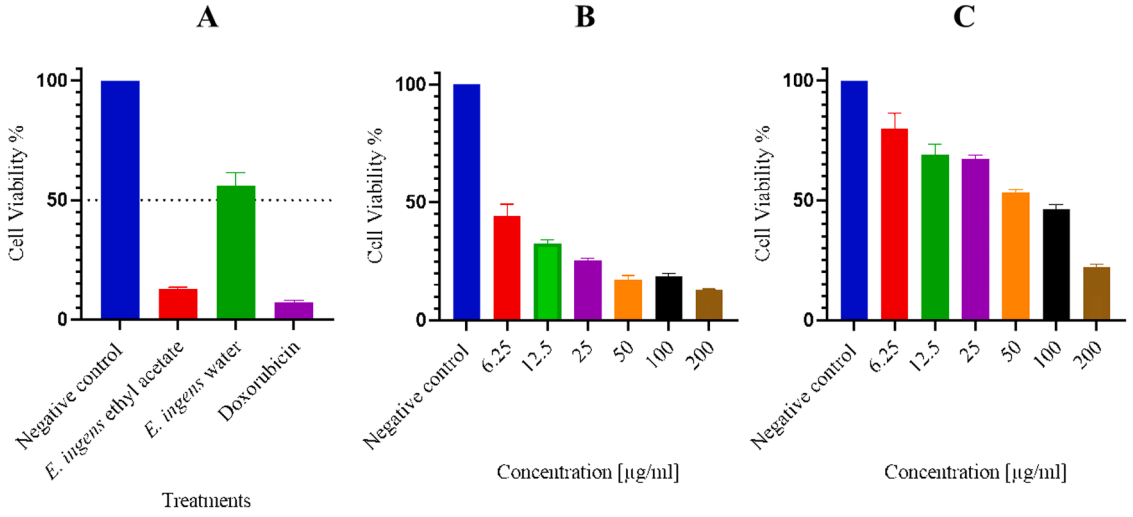

Fig. 1. (A). Screening for cellular proliferation inhibition of DU-145 by *E. ingens* fractions: Inhibition of cellular proliferation at a 200 μg/ml concentration by the water and ethyl acetate extract fractions of *E. ingens* on DU-145.; doxorubicin at 200 μg/ml was used as a positive control, and 0.2 % DMSO as a negative control; (B). Inhibition of cellular proliferation by *E. ingens* ethyl acetate fraction: Inhibition of cellular proliferation by *E. ingens* ethyl acetate fraction on serial concentrations 2-fold dilution on DU-145 so as to determine IC_{50}; (C). Cellular safety: The potential cellular safety of *E. ingens* ethyl acetate extract fraction was determined using non-cancerous Vero E6, whereby cells were treated with 2-fold serial dilution of the *E. ingens* ethyl acetate extract fraction so as to determine the CC_{50}. All treatments lasted for 48 h and were done in triplicate ($n = 3$); values were expressed as Mean ± SEM.

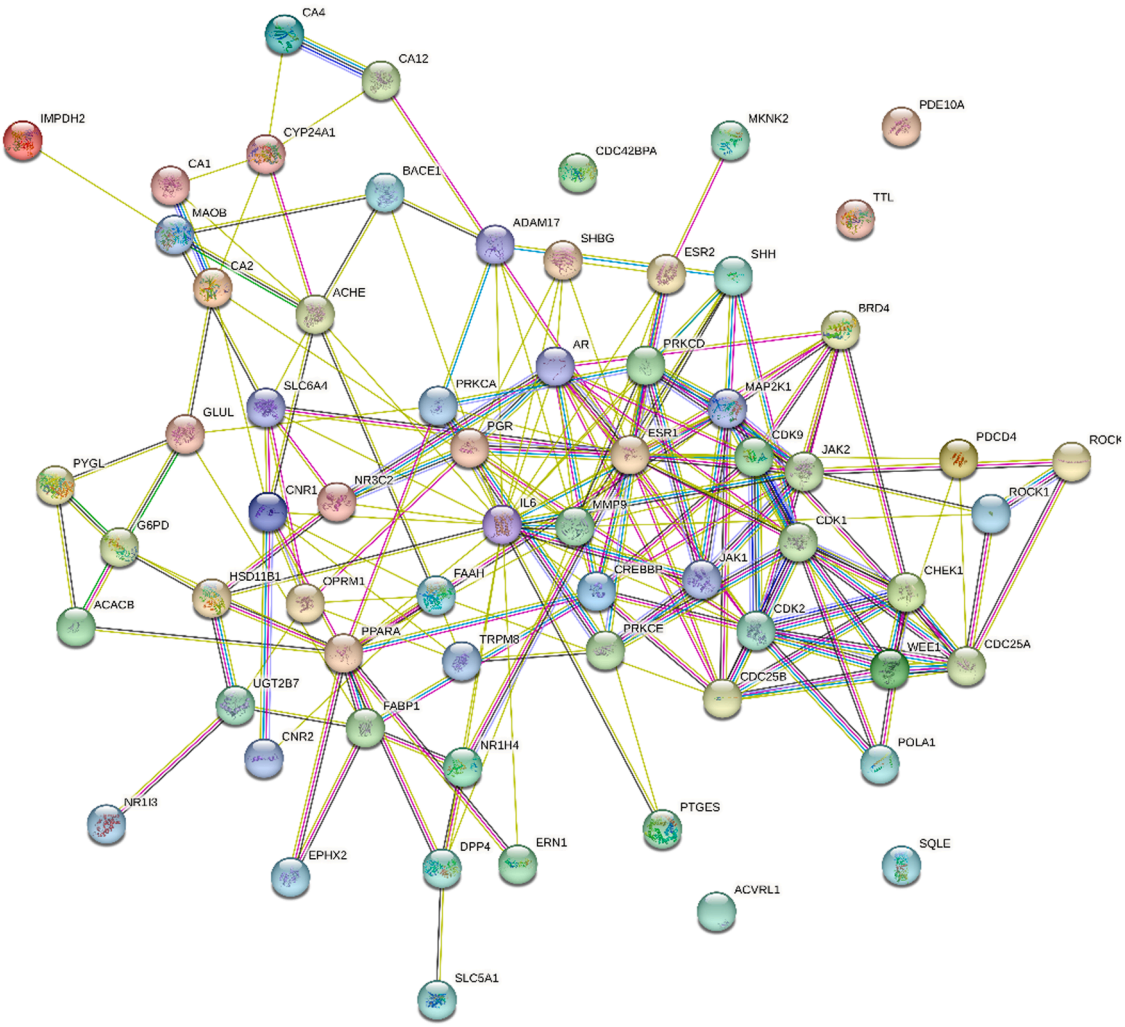

Fig. 2. PPI network of the key targets in *E. ingens* ethyl acetate action against human prostate cancer cells.

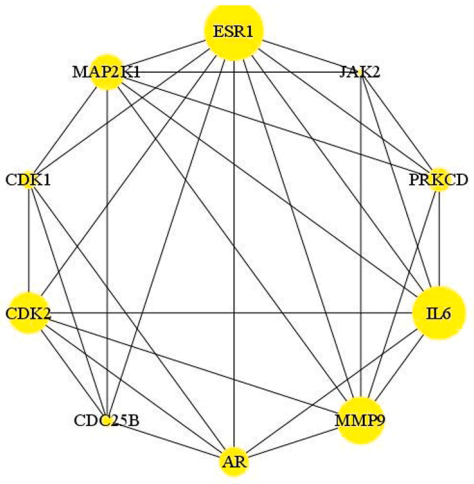

Fig. 3. Obtained ten hub genes. The larger the node is, the more important the target in the network.

Table 2
The GC–MS identified compounds from *E. ingens* ethyl acetate fraction.

Peak Nr.	Rt (min)	Compound identified	Peak Area %	MW (g/mol)	MF	Structure Type
1.	5.302	1-decene	0.29	140	$C_{10}H_{20}$	Alkene
2.	7.952	Bicyclo[3.1.1]heptan-3-ol	0.23	152	$C_{10}H_{16}O$	Terpenoid
3.	8.381	1-dodecene	2.11	168	$C_{12}H_{24}$	Alkene
4.	9.034	Bicyclo[3.1.1]hept-3-en-2-one	0.25	150	$C_{10}H_{14}O$	Terpenoid
5.	11.339	1-tridecene	3.64	182	$C_{13}H_{26}$	Alkene
6.	13.123	2,4-di-tert-butylphenol	2.03	206	$C_{14}H_{22}O$	Phenol
7.	14.003	1-octadecene	4.05	252	$C_{18}H_{36}$	Alkene
8.	14.003	1-octadecene	4.05	252	$C_{18}H_{36}$	Alkene
9.	18.543	1-heneicosanol	1.86	312	$C_{21}H_{44}O$	Fatty alcohol
10.	18.543	1-heneicosanol	1.86	312	$C_{21}H_{44}O$	Fatty alcohol
11.	18.543	1-heneicosanol	1.86	312	$C_{21}H_{44}O$	Fatty alcohol
12.	24.128	Octadecyl trifluoroacetate	0.37	366	$C_{20}H_{37}F_3O_2$	Fatty Acid
13.	24.639	Prasterone	0.14	288	$C_{19}H_{28}O_2$	Sterol
14.	25.177	Andrographolide	1.22	350	$C_{20}H_{30}O_5$	Diterpenoid
15.	25.695	Ferruginol	0.13	286	$C_{20}H_{30}O$	Diterpenoid
16.	25.834	(1R,7S,E)−7-isopropyl-4,10-dimethylenecyclodec-5-enol	0.63	220	$C_{15}H_{24}O$	Sesquiterpenoid
17.	26.079	2-bornanol	16.75	348	$C_{16}H_{20}N_4O_5$	Terpenoid
18.	26.435	11-oxoandrosterone	1.53	376	$C_{22}H_{36}O_3Si$	Sterol
19.	26.933	Squalene	0.20	410	$C_{30}H_{50}$	Triterpenoid
20.	28.535	6-pentylidene-4,5-secoandrostane-4,17.beta.-diol	55.39	362	$C_{24}H_{42}O_2$	Sterol
21.	28.827	17.beta.--hydroxy-6.alpha.-pentyl-4-nor-3,5-secoandrostan-3-oic acid, methyl ester	1.78	378	$C_{24}H_{42}O_3$	Fatty acid methyl ester
22.	28.827	17.beta.--hydroxy-6.alpha.-pentyl-4-nor-3,5-secoandrostan-3-oic acid, methyl ester	1.78	378	$C_{24}H_{42}O_3$	Fatty acid methyl ester

Key: Rt, retention time; MW, Molecular Weight; MF, Molecular Formula.

chromatogram, comprising 18 compounds (Table 2), mostly terpenoids. The most abundant compounds include 6-pentylidene-4,5-secoandrostane-4,17.beta.-diol (55.39 %), 2-bornanol (16.75 %) and 1-octadecene, which appears twice to make up 8.1 %.

In silico work

Screening for drug-like compounds in E. ingens ethyl acetate fraction

Detailed results on the drug candidate screening of the 18 *E. ingens* ethyl acetate compounds identified through GC–MS analysis (Table 2) are shown in supplementary table 3. Out of the 18 compounds, only 7 were considered ideal drug-like candidates. The prioritized 7 compounds are 1-dodecene, 1-heneicosanol, 1-octadecene, octadecyl trifluoroacetate, andrographolide, and squalene.

Targets of E. ingens ethyl acetate prioritized drug-like compounds and therapeutic targets for prostate cancer

From the SWISS TargetPrediction (STP) and BindingDB (BDB) databases, a total of 87 potential targets were identified as targets for the 7 prioritized *E. ingens* ethyl acetate compounds (supplementary table 4). 76 total targets were retained after removing duplicates. Additionally, we retrieved a total of 12,674, and 4389 target genes that are closely related to PCa from GeneCards and DisGenet, respectively. A total of 12,889 genes were identified after duplicates were eliminated (supplementary table 5). Gene datasets obtained from the 76 *E. ingens* ethyl acetate-related targets and the 12,889 PCa-related targets which were imported into an online Venn diagram, overlapped, and a total of 65 intersecting targets were obtained. The analyzed relationship of gene targets between *E. ingens* ethyl acetate (drug) and disease resulted in 65 intersection genes (key targets) shown in supplementary figure 5, and further details of the targets are presented in supplementary table 6.

Compound-disease target protein–protein interaction (PPI) network

A total of 65 key genes were obtained by mapping the *E. ingens* ethyl acetate targets to the PCa disease targets. The 65 targets were imported into the STRING database and imported into Cytoscape for visualization and analysis, and a network consisting of 65 nodes and 195 edges was obtained (Fig. 2). The average node degree is 6 and the average local clustering coefficient is 0.48; the PPI enrichment p-value was $< 1.0e\text{-}16$; thus, proteins have more interactions among themselves than would be expected for a random set of proteins of similar size drawn from the genome. Such a significant enrichment indicated that the proteins are at least partially biologically connected as a group. TTL, ACVRL1, PDE10A, and SQLE were left out of the PPI network analysis as they have no interaction with other proteins. In the network, the top ten targets with the highest Maximal Clique Centrality (MCC) scores were estrogen receptor alpha (ESR1), interleukin-6 (IL6), matrix metalloproteinase 9 (MMP9), cyclin-dependent kinase 2 (CDK2), mitogen-activated protein kinase 1 (MAP2K1), androgen receptor (AR), protein kinase C delta (PRKCD), cyclin-dependent kinase 1 (CDK1), Cell Division Cycle 25B (CDC25B), and tyrosine-protein kinase JAK2 (Fig. 3).

GO and KEGG pathway enrichment

The 65 key targets of *E. ingens* ethyl acetate against PCa were enriched in 1418 GO (gene ontology) terms, including 1000 for

biological processes (BP) terms, 107 for cellular component (CC) terms, and 311 for molecular functions (MF) terms ($p < 0.05$). The top 20 significant GO terms for each category are shown in the dot plot chart (supplementary figures 6A-C). The y-axis represents the enriched categories, and the x-axis represents the number of enrichments. The order of importance was ranked from top to bottom by −Log10 (p value). GO analysis showed that the key targets mainly play a role in the biological processes of responding to oxygen-containing compounds, lipids and organic cyclic compounds. CC was mainly enriched in the membrane raft, membrane micro-domain, and cyclin-dependent protein kinase holoenzyme complex. MF analysis associated the key targets with protein kinase, phosphotransferase and nuclear receptor activities. KEGG (Kyoto Encyclopedia of Genes and Genomes) signaling pathway analysis indicated that the key targets were significantly enriched in 170 pathways, the top 20 signaling pathways were screened by - LogP values (supplementary figure 7A), and the prostate cancer pathway was selected for analysis as the most relevant molecular pathways affected by *E. ingens* ethyl acetate inhibition of prostate cancer cells (supplementary figure 7B).

Gene expression analysis

The mRNA expression of AR, CDK1, p53, BCL-2, and Caspase-3 was determined by RT-qPCR to validate the top putative molecular targets of *E. ingens* ethyl acetate in prostate cancer cells as demonstrated by network pharmacology (Fig. 3). AR and CDK1 were among the ten hub genes. Further, we picked the p53, BCL-2, and caspase-3 genes due to their role in apoptosis and considering many anticancer drugs work by inducing apoptosis. The quantification cycle, also known as the threshold cycle (Ct), was calculated, and relative mRNA expression levels of target genes were normalized to β-actin using the $2^{-\Delta\Delta Ct}$ method. The results are presented in Fig. 4.

There was significant downregulation of AR ($p = 0.0129$) and BCL-2 ($p = 0.0002$, relative fold change recorded was 5.0). Furthermore, while significant upregulation was also observed in the expression level of p53 ($p < 0.0001$, relative fold change of 2.5), there was no significant difference in the upregulation of caspase 3 ($p = 0.1004$). Though CDK1 was observed to be upregulated, the RT-qPCR results still allude to the fact that the *E. ingens* ethyl acetate fraction interfere with prostate cancer cells proliferation by inducing apoptosis.

Discussion

Active surveillance, surgery, radiotherapy, hormonal therapy, immunotherapy, and chemotherapy are treatment options currently available for prostate cancer. These options have their limitations, particularly the accompanying adverse side effects. Hence, the need to search for an effective and safe treatment alternative. Cancer cells exhibit sustained proliferation and resistance to cell death, and thus, compounds that can stop or slow down cell proliferation in rapidly dividing cells hold great promise as anticancer therapeutics. Natural products provide an outlet for the identification of promising new anticancer agents that are highly efficient with low toxicity.

Based on the cell-based MTT assay, our findings demonstrated significant antiproliferative effects of ethyl acetate fraction of *E. ingens* roots on the DU-145 prostate cancer cell lines without affecting the non-cancerous cells (Vero E6). An $IC_{50} < 30$ µg/ml is one of the established criteria by the US National Cancer Institute (NCI) to consider a crude extract promising and to be considered for purification [21]. Interestingly, we observed that the ethyl acetate fraction of *E. ingens* caused cytotoxicity in DU-145 with an IC_{50} value that was less than 10 µg/ml. A drug with a low IC_{50} value is effective at low concentrations and will therefore exhibit less systemic toxicity when administered. Therefore, *E. ingens* ethyl acetate fraction seems to be a potential source for prospecting chemotherapeutic agent against PCa. The inhibitory effect of *E. ingens* ethyl acetate on DU-145 was more potent when compared to that reported for longifolene isolated from *Chrysopogon zizanioides* (IC_{50} of 78.64 µg/mL) on the same DU-145 cells [22]. In prior studies, the stem and leaf parts of *E. ingens* were inactive against human colon adenocarcinoma (CACO2), human hepatoma (HepG2), and human breast adenocarcinoma (MCF-7) cell lines [10]. This might be related to the difference in the plant's parts or the extraction solvents that were used. While El-Hawary et al. [10] used the methanolic extract of the plant, we tested the ethyl acetate fraction of the crude (dichloromethane-methanol) extract. A different set of chemical compounds were likely to be present in the test samples; therefore, a future study to investigate the cytotoxic effect of the root ethyl acetate fraction of *E. ingens* on the CACO2, HepG2, and MCF-7 cell lines is recommended.

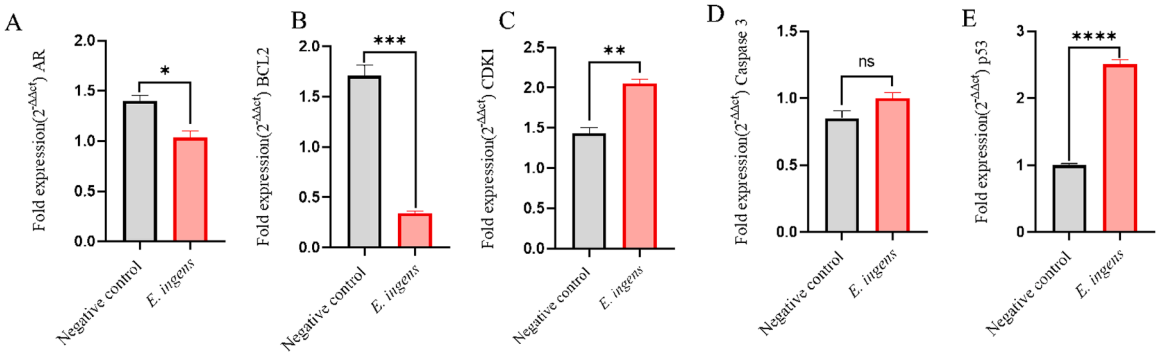

Fig. 4. Relative gene expression analysis of *E. ingens* ethyl acetate treated DU-145 cells and the untreated control (0.2 % DMSO). (A) AR, (B) BCL-2, (C) CDK1, (D) caspase-3 and (E) p53. *ns $p > 0.05$, * $p \leq 0.05$, ** $p \leq 0.01$, *** $p \leq 0.001$, **** $p \leq 0.0001$* as compared to untreated control.

A drug with a measure of the safety margin (selectivity index) of >3 is considered highly selective [14]. The ethyl acetate fraction of *E. ingens* had an SI greater than 3, an indicator of high selectivity for the cancer cells, which implies that the plant fraction was not linked with cellular toxicity, as demonstrated in prior research [8].

The findings of this study depict a high abundance of terpenoids, which restrict the cell cycle in cancer cells through the induction of apoptosis [4]. Flavonoids are known antioxidants under normal conditions and potent pro-oxidants in cancer cells. Together with phenols, tannins, saponins, and sterols, they arrest the cell cycle, induce apoptosis, and suppress cancer cell proliferation and invasiveness [4]. Furthermore, some of the GC–MS-identified compounds in this study have been reported to elicit anticancer activity. For example, andrographolide, a diterpenoid isolated from *Andrographis paniculata* Nees, induced cell cycle arrest and apoptosis in HT-29 human colon cancer cells [4]. By increasing intracellular reactive oxygen species, squalene induces anti-proliferative activity against ovarian, breast, lung, and colon cancers [23]. Given that these compounds are found in the ethyl acetate fraction of *E. ingens*, we suggest that they may be responsible for the demonstrated antiproliferative effects of the plant on DU-145. Further research is required to isolate these compounds and evaluate their antiproliferative activity on prostate cells.

Network pharmacology is currently used in cancer therapy to develop new drugs. The multi-target pathway application of network pharmacology is widely adopted to study the mechanism of action of traditional medicine; it identifies the active ingredients of plants, predicts their targets, and subsequently combines them with disease targets to generate a presentable drug-target-disease relationship. We selected 7 GC–MS-identified compounds with good absorption, distribution, metabolism, and excretion (ADME) activity using the RO5, as well as the blood–brain barrier, total polar surface area, CYP2D6, and CYP3A4. Drug screening and development rely heavily on pharmacokinetic characteristics. Without appropriate pharmacokinetic qualities, drugs will fail to attain the requisite concentration in the target organs needed to produce therapeutic effects [24]. The candidate targets of the selected *E. ingens* ethyl acetate bioactive compounds for prostate cancer treatment were obtained, of which ESR1, IL6, MMP9, CDK2, MAP2K1, AR, PRKCD, CDK1, CDC25B, and JAK2 were at the core positions in the PPI network. These genes are considered possible molecular targets of *E. ingens* ethyl acetate against prostate cancer cells. The MMPs family is known to have proteolytic effects on the cell membrane; member proteins such as MMP9 release proangiogenic factors, which act on endothelial cells to induce cell migration and proliferation. An increased level of MMP9 causes metastasis in androgen-independent prostate cancer [25]. There have been reports on the role of ESR1, PRKCD, and IL6 in the proliferation and migration of PCa cells, and inhibitors of JAK2 have been suggested to be imperative in the treatment of advanced PCa [26–29]. Targeted inhibition of MAP2K1 expression elicits cell apoptosis and weakens cell proliferation in DU-145 and PC-3 prostate cancer cells [30]. The cell cycle protein-dependent kinase (CDK) and cell cycle proteins, as well as CDK inhibitors, are essential in the regulation of the cell cycle; hence, impairment in the activities of these cell cycle mediators is observed in many types of cancer. CDK2 is a core regulator of the cell cycle through late G1-phase and S-phase. CDK2 is thought to be strongly linked to the development of cancer, and accumulating evidence shows that inhibition of CDK2 induces cancer cell apoptosis without cellular damage [31]. CDC25B is a cell cycle transition regulatory enzyme; and an important target of the checkpoint machinery in maintaining genome stability during DNA damage [32]. Overexpression of CDC25B has been reported in many types of human cancers, and targeted cellular depletion of the enzyme in DU-145 facilitated rapamycin anticancer effects [33]. Given the clear evidence that these genes are involved in the development and progression of prostate cancer, the ability to modulate them might have contributed to the observed antiproliferative property of the ethyl acetate fraction of *E. ingens*.

The prostate cancer pathway was selected for analysis; the pathway showed a set of multiple pathways through which the therapeutic effect of *E. ingens* ethyl acetate on prostate cancer may be produced; these include the PI3K/Akt, MAPK, and p53 signaling pathways. The phosphatidylinositol-3 kinase (PI3K)/protein kinase B (Akt) signaling pathway is an important tumor cell pathway that participates in the occurrence, invasion, and distant metastasis of prostate cancer. Long-term ADT can abnormally activate the PI3K/Akt pathway, thereby enhancing the antiapoptotic ability of tumors [34]. Therefore, the PI3K/Akt pathway, could be an important potential target of the non-AR pathway in the treatment of PCa. Mitogen-activated protein kinases (MAPKs) are serine-threonine kinases that could link extracellular signals to fundamental cellular processes such as cell growth, proliferation, differentiation, migration, and apoptosis. The p53 pathway is one of the crucial signaling pathways for cancer cell apoptosis. As a cancer suppressor gene, p53 regulates the downstream genes and plays a part in DNA repair, cell cycle regulation, and apoptosis. Hence, reactivation and restoration of p53 function hold great potential for the treatment of PCa.

Multiple lines of evidence in the field of cancer research have demonstrated the role of secondary metabolites in natural products in influencing significant transcription factors involved in carcinogenesis. We used RT-qPCR to validate the predicted molecular targets of *E. ingens* in prostate cancer. AR signaling plays a crucial role in the growth of normal prostate tissue and PCa pathogenesis and progression. In advanced PCa stages, AR mutations and overexpression contribute to sustained proliferation [35]. Overexpression of CDK1 promotes PCa progression, and when this kinase is hyperactivated, it mediates the phosphorylation that activates AR when there are no ligands [36,37]. The treatment of DU-145 prostate cancer cells with *E. ingens* ethyl acetate resulted in a significant downregulation of AR when compared with the untreated control. However, *E. ingens* ethyl acetate showed upregulation in the expression of CDK1. This unusual finding was also observed by Mustafa et al. [38]. CDK1 is known to be capable of avoiding an accumulation of oncogenic mutations during cell division, which might explain the result [39]. In cancer cells, the evasion of cell death is often achieved by upregulating anti-apoptotic proteins like BCL-2 or impairing the function of pro-apoptotic proteins such as caspase-3. BCL-2 controls the mitochondrial apoptotic pathway by binding to pro-apoptotic proteins and preventing pore formation and cytochrome c release. Apoptosis is executed by caspases and various upstream regulatory factors, including p53. We observed an upregulation in the expression of caspase-3 and p53 with concomitant downregulation of BCL-2 when *E. ingens* ethyl acetate-treated prostate cancer cells were compared with the untreated prostate cancer cells. A recent computational study revealed that flavonoids, found to be abundant in our study, have strong interactions with caspase-3, BCL-2, and p53 [40]. AR, p53, BCL-2, and caspase-3 are involved in the PI3K/Akt, MAPK, and p53 signaling pathways, the difference in their expression level, found between the *E. ingens*

ethyl acetate-treated human prostate cancer cells and the untreated cells justifies the network pharmacology predictions. The results suggest that *E. ingens* ethyl acetate's antiproliferative activity is likely to be exhibited by regulating the pathways to cause induction of apoptosis as well as suppression of cell cycle.

Conclusion

The ethyl acetate fraction of *E. ingens* exhibited antiproliferative activity against prostate cancer cells. As pointed out by network pharmacology analyses, drug-like compounds of *E. ingens* ethyl acetate namely, 1-dodecene, 1-heneicosanol, 1-octadecene, octadecyl trifluoroacetate, andrographolide, and squalene, targeted ESR1, IL6, MMP9, CDK2, MAP2K1, AR, PRKCD, CDK1, CDC25B, and JAK2. The most likely molecular mechanism of action of the compounds was suggested to be the regulation of the PI3K/Akt, MAPK, and p53 signaling pathways. Interestingly, the expression levels of AR, p53, caspase-3, and BCL-2 were reversed in *E. ingens* ethyl acetate-treated prostate cancer cells when they were compared with the untreated cancer cells. An additional use of other prostate cancer cell lines (PC3 and LNCaP) might have added to the robustness of our data; this was considered a limitation of this study. Nonetheless, for the first time, to the best of our knowledge, we have demonstrated that *E. ingens* ethyl acetate extract fraction could be a potential source of a new, effective, and safe alternative therapeutic option to the current prostate cancer treatments. However, additional *in vivo* research as well as testing in multiple cancer cell lines is necessary to better enhance the potential clinical use of the plant.

Funding

This work was supported by the African Union scholarship program through the Pan African University Institute for Basic Sciences, Technology, and Innovation (PAUSTI) funding to **Innocent Oluwaseun Okpako**, REF: PAU/ADM/PAUSTI/2020/8; and the KEMRI Internal Research Grant funding to **Sospeter Ngoci Njeru**, REF: KEMRI/IRG/EC0017.

CRediT authorship contribution statement

Innocent Oluwaseun Okpako: Conceptualization, Methodology, Funding acquisition, Investigation, Formal analysis, Data curation, Writing – original draft. **Florence Atieno Ng'ong'a:** Conceptualization, Supervision, Resources, Writing – review & editing. **Cleophas Mutinda Kyama:** Conceptualization, Supervision, Writing – review & editing. **Sospeter Ngoci Njeru:** Conceptualization, Methodology, Supervision, Validation, Resources, Writing – review & editing.

Declaration of Competing Interest

The authors declare that they have no known competing financial interests or personal relationships that could have appeared to influence the work reported in this paper.

Acknowledgments

We acknowledge PAUSTI, the center for Traditional Medicine and Drug Research, Kenya Medical Research Institute (KEMRI), and Jomo Kenyatta University of Agriculture and Technology for provision of laboratories and resources. We are also grateful to John Chukwuma Oyem for proofreading the draft article.

Supplementary materials

Supplementary material associated with this article can be found, in the online version, at doi:10.1016/j.sciaf.2023.e01943.

References

[1] H. Sung, J. Ferlay, R.L. Siegel, M. Laversanne, I. Soerjomataram, A. Jemal, F. Bray, Global Cancer Statistics 2020: GLOBOCAN Estimates of incidence and mortality worldwide for 36 cancers in 185 countries, CA Cancer J. Clin. 71 (3) (2021) 209–249, https://doi.org/10.3322/caac.21660.

[2] F. Bray, D.M. Parkin, F. Gnangnon, G. Tshisimogo, J.F. Peko, I. Adoubi, M. Assefa, L. Bojang, B. Awuah, M. Koulibaly, N. Buziba, A. Korir, C. Dzamalala, B. Kamate, S. Manraj, J. Ferro, C. Lorenzoni, R. Hansen, H. Nouhou, T. Chingonzoh, Cancer in sub-Saharan Africa in 2020: a review of current estimates of the national burden, data gaps, and future needs, Lancet Oncol. 23 (6) (2022) 719–728, https://doi.org/10.1016/S1470-2045(22)00270-4.

[3] K. Okaiyeto, O.O. Oguntibeju, African herbal medicines: adverse effects and cytotoxic potentials with different therapeutic applications, Int. J. Environ. Res. Public Health 18 (5988) (2021), https://doi.org/10.3390/IJERPH18115988.

[4] J. Iqbal, B.A. Abbasi, T. Mahmood, S. Kanwal, B. Ali, S.A. Shah, A.T. Khalil, Plant-derived anticancer agents: a green anticancer approach, Asian Pac. J. Trop. Biomed. 7 (12) (2017) 1129–1150.

[5] V. Jain, A. Dudhal, R. Chitale, P. Bankar, A survey of some medicinally important plants of the family euphorbiaceae from Baramati area of Pune district of Maharashtra, India, Prasad. Bankar. 6 (4) (2021) 456–462.

[6] S. Koduru, D.S. Grierson, A.J. Afolayan, Ethnobotanical information of medicinal plants used for treatment of cancer in the Eastern Cape Province, South Africa, Curr. Sci. 92 (7) (2017) 906–908.

[7] M.A. Kena, Antifungal activities of *Monsonia burkeana* and *Euphorbia ingens* extracts against *Penicillium digitatum*, the causal agent of citrus green mould, Afr. Plant Prot. 19 (2016) 1–3, https://doi.org/10.10520/EJC188537.

[8] S.N. Njeru, M.A. Obonyo, Potency of extracts of selected plant species from Mbeere, Embu County-Kenya against *Mycobacterium tuberculosis*, J. Med. Plant. Res. 10 (12) (2016) 149–157, https://doi.org/10.5897/jmpr2016.6044.

[9] M.J. Ross, G.J. Steyn, Preliminary results on the ichthyocidal properties of *Euphorbia ingens* (*Euphorbiaceae*), Afr. J. Aquat. Sci. 29 (2) (2004) 265–269, https://doi.org/10.2989/16085910409503819.

[10] S.S. El-Hawary, R. Mohammed, A.F. Tawfike, N.M. Lithy, S.F. Abouzid, M.N. Amin, U.R. Abdelmohsen, E. Amin, Cytotoxic activity and metabolic profiling of fifteen *Euphorbia* species, Metabolites 11 (1) (2020) 15, https://doi.org/10.3390/METABO11010015.

[11] R. Beesoo, V.S. Neergheen, R. Bhagooli, A.-M. Reid, I.A. Lambrechts, L. Gibango, D. Bodiba, N. Lall, T. Bahorun, *In vitro* antioxidant, antibacterial, cytotoxic, and epigenetic screening of crude extract and fractions of the marine sponge *Neopetrosia exigua* from Mauritius waters, Sci. Afr. (2023) e01867, https://doi.org/10.1016/j.sciaf.2023.e01867.

[12] F. Souleymane, K.K. Benjamin, D. Ollo, Y.R. Serge, I. Sylvain, O. Noufou, O. Moussa, G.I. Pierre, Acute and subchronic toxicity assessment of the dichloromethane /methanol stem bark extract from *Erythrina senegalensis* DC (*Fabaceae*) in Wistar rats, Issu. Biolog. Sci. Pharmaceut. Res. 9 (1) (2021) 19–26.

[13] T.K. Kim, J.H. Lee, H.I. Yong, M.C. Kang, J.Y. Cha, J.Y. Chun, Y.S. Choi, Effects of defatting methods on the physicochemical properties of proteins extracted from *Hermetia illucens* larvae, Foods 11 (10) (2022), https://doi.org/10.3390/foods11101400.

[14] Q. Eghianruwa, O. Osoniyi, S. Wachira, N. Maina, R. Mbugua, M. Imbuga, *In vitro* antiproliferative studies of extracts of the marine molluscs: *Tympanatonus fuscatus* Var radula (linnaeus) and *Pachymelania aurita* (muller), Int. J. Biochem. Mol. Biol. 10 (1) (2019) 1–8.

[15] A.R. Lima, A.M. Araújo, J. Pinto, C. Jerónimo, R. Henrique, M. Bastos, L. de, M. Carvalho, P. Guedes de Pinho, Discrimination between the human prostate normal and cancer cell exometabolome by GC-MS, Sci. Rep. 8 (1) (2018) 5539, https://doi.org/10.1038/s41598-018-23847-9.

[16] S. Sergazy, A. Vetrova, I.E. Orhan, F.S. Senol Deniz, A. Kahraman, J.Y. Zhang, M Aljofan, Antiproliferative and cytotoxic activity of *Geraniaceae* plant extracts against five tumor cell lines, Futu. Sci. OA 8 (2) (2022), https://doi.org/10.2144/fsoa-2021-0109.

[17] J.R. Shaikh, M. Patil, Qualitative tests for preliminary phytochemical screening: an overview, Int. J. Chem. Stud. 8 (2) (2020) 603–608.

[18] N. Patel, L.N. Patel SmtSSPatel, N.B. Patel, L.N. Patel, K.D. Patel, M.V. Patel, H.S. Kalasariya, ADMET & Cytotoxicity prediction of red seaweed Gracillaria dura: an in silico approach, Artic. World J. Pharmaceut. Res. 9 (3) (2020) 991–1004, https://doi.org/10.20959/wjpr20203-16872.

[19] M. Navid, S. Rad, S. Behrouz, S. Aghajani, M. Behrouz, E. Zarenezhad, A. Ghanbariasad, Design, synthesis, anticancer and *in silico* assessment of 8-caffeinyl-triazolylmethoxy hybrid conjugates, RSC Adv. 13 (5) (2023) 3056–3070, https://doi.org/10.1039/D2RA07683G.

[20] C.H. Chin, S.H. Chen, H.H. Wu, C.W. Ho, M.T. Ko, C.Y. Lin, CytoHubba: identifying hub objects and sub-networks from complex interactome, BMC Syst. Biol. 8 (4) (2014) S11, https://doi.org/10.1186/1752-0509-8-S4-S11.

[21] I. Canga, P. Vita, A.I. Oliveira, M.Á. Castro, C. Pinho, *In vitro* cytotoxic Activity of African plants: a review, Molecules 27 (15) (2022) 1–18, https://doi.org/10.3390/molecules27154989.

[22] M. Grover, T. Behl, T. Virmani, M. Sanduja, H.A. Makeen, M. Albratty, H.A. Alhazmi, A.M. Meraya, S.G. Bungau, Exploration of cytotoxic potential of Longifolene/Junipene isolated from *Chrysopogon zizanioides*, Molecules 27 (18) (2022) 5764, https://doi.org/10.3390/molecules27185764.

[23] M.A. Lozano-Grande, S. Gorinstein, E. Espitia-Rangel, G. Dávila-Ortiz, A.L. Martínez-Ayala, Plant sources, extraction methods, and uses of squalene, Int. J. Agro. 2018 (2018) 1–13, https://doi.org/10.1155/2018/1829160.

[24] S. Tian, J. Wang, Y. Li, D. Li, L. Xu, T. Hou, The application of in silico drug-likeness predictions in pharmaceutical research, Adv. Drug Deliv. Rev. 86 (2015) 2–10.

[25] K.C. Chen, C.C. Peng, C.H. Peng, C.L. Hsieh, R.Y. Peng, The aqueous soluble polyphenolic fraction of *Psidium guajava* leaves exhibits potent anti-angiogenesis and anti-migration actions on DU145 cells, Evid.-Based Complement. Altern. Med. 2011 (2011) 8, https://doi.org/10.1093/ECAM/NEQ005.

[26] P. Beinhoff, L. Sabharwal, V. Udhane, C. Maranto, P.S. LaViolette, K.M. Jacobsohn, S. Tsai, K.A. Iczkowski, L. Wang, W.A. Hall, S.M. Dehm, D. Kilari, M. T. Nevalainen, Second-generation Jak2 inhibitors for advanced prostate cancer: are we ready for clinical development? Cancers (Basel) 13 (20) (2021) https://doi.org/10.3390/cancers13205204.

[27] S. Chen, K. Lu, Y. Hou, Z. You, C. Shu, X. Wei, T. Wu, N. Shi, G. Zhang, J. Wu, S. Chen, L. Zhang, W. Li, D. Zhang, S. Ju, M. Chen, B. Xu, YY1 complex in M2 macrophage promotes prostate cancer progression by upregulating IL-6, J. Immunother. Cancer 11 (4) (2023), e006020, https://doi.org/10.1136/jitc-2022-006020.

[28] U. Jariwala, J. Prescott, L. Jia, A. Barski, S. Pregizer, J.P. Cogan, A. Arasheben, W.D. Tilley, H.I. Scher, W.L. Gerald, G. Buchanan, G.A. Coetzee, B. Frenkel, Identification of novel androgen receptor target genes in prostate cancer, Mol. Cancer 6 (1) (2007) 39, https://doi.org/10.1186/1476-4598-6-39.

[29] A. Palicelli, S. Croci, A. Bisagni, E. Zanetti, D. De Biase, B. Melli, F. Sanguedolce, M. Ragazzi, M. Zanelli, A. Chaux, What do we have to know about PD-L1 expression in prostate cancer? A systematic literature review (part 6): correlation of PD-L1 expression with the status of mismatch repair system, BRCA, PTEN, and other genes, Biomedicines 10 (2) (2022) 236.

[30] J.Y. Zhang, Y.N. Li, X. Mu, Z.L. Pan, W.B. Liu, Targeted regulation of miR-195 on MAP2K1 for suppressing ADM drug resistance in prostate cancer cells, Eur. Rev. Med. Pharmacol. Sci. 22 (24) (2018) 8599–8608, https://doi.org/10.26355/EURREV_201812_16623.

[31] S. Tadesse, A.T. Anshabo, N. Portman, E. Lim, W. Tilley, C.E. Caldon, S. Wang, Targeting CDK2 in cancer: challenges and opportunities for therapy, Drug Discov. Today 25 (2) (2020) 406–413, https://doi.org/10.1016/J.DRUDIS.2019.12.001.

[32] R. Boutros, V. Lobjois, B. Ducommun, CDC25 phosphatases in cancer cells: key players? Good targets? Nat. Rev. Cancer 7 (7) (2007) 495–507, https://doi.org/10.1038/nrc2169.

[33] R.Q. Chen, Q.K. Yang, B.W. Lu, W. Yi, G. Cantin, Y.L. Chen, C. Fearns, J.R. Yates, J.D. Lee, CDC25B mediates rapamycin-induced oncogenic responses in cancer cells, Cancer Res. 69 (6) (2009) 2663–2668, https://doi.org/10.1158/0008-5472.CAN-08-3222/654700/P/CDC25B-MEDIATES-RAPAMYCIN-INDUCED-ONCOGENIC.

[34] C. Pisano, M. Tucci, R.F. Di Stefano, F. Turco, G.V. Scagliotti, M. Di Maio, C. Buttigliero, Interactions between androgen receptor signaling and other molecular pathways in prostate cancer progression: current and future clinical implications, Crit. Rev. Oncol. Hematol. 157 (2021), 103185, https://doi.org/10.1016/J.CRITREVONC.2020.103185.

[35] K. Hatano, N. Nonomura, Systemic therapies for metastatic castration-resistant prostate cancer: an updated review, World J. Men. Health 41 (2023), https://doi.org/10.5534/WJMH.220200.

[36] X.T. Gao, J. Liang, L.Y. Wang, Z. Zhang, P. Yuan, J. Wang, Y. Gao, F. Ma, C. Calagua, H. Ye, O. Voznesensky, S. Wang, T. Wang, J. Liu, S. Chen, X. Liu, Phosphorylation of the androgen receptor at Ser81 is co-sustained by CDK1 and CDK9 and leads to AR-mediated transactivation in prostate cancer, Mol. Oncol. 15 (7) (2021) 1901–1920, https://doi.org/10.1002/1878-0261.12968.

[37] Y. Huang, S. Lu, Y. Chen, Y. Qing, R. Wu, T. Ma, Z. Zhang, Y. Wang, K. Li, Verification of cell cycle-associated cyclin-dependent kinases facilitated prostate cancer progression by integrated bioinformatic analysis and experimental validation, Heliyon 8 (8) (2022) e10081, https://doi.org/10.1016/J.HELIYON.2022.E10081.

[38] K. Mustafa, H. Mohamed, A.M. Shah, S. Yu, M. Akhlaq, H. Xiao, S. Li, T. Naz, S. Nosheen, X. Bai, *In vitro* anticancer potential of *Berberis lycium* Royle extracts against human hepatocarcinoma (HepG2) cells, Biomed. Res. Int. 2020 (2020).

[39] M. Malumbres, M. Barbacid, Cell cycle, CDKs and cancer: a changing paradigm, Nat. Rev. Cancer 9 (3) (2009) 153–166.

[40] S.C. Wong, M.N.A. Kamarudin, R. Naidu, Anticancer mechanism of flavonoids on high-grade adult-type diffuse gliomas, Nutrients 15 (4) (2023), https://doi.org/10.3390/NU15040797.